10th ICARD IMWA 2015 | 10th International Conference on Acid Rock Drainage & IMWA Annual Conference

Diavik Waste Rock Project: Reactive Transport Simulation of Sulfide Weathering

David Wilson[1], Richard Amos[2], David Blowes[1], Jeff Langman[1], David Sego and Leslie Smith

1. *Department of Earth and Environmental Sciences, University of Waterloo, Canada*
2. *Department of Earth Sciences, Carleton University, Canada*
3. *Department of Civil and Environmental Engineering, University of Alberta, Canada*
4. *Department of Earth, Ocean and Atmospheric Sciences, University of British Columbia, Canada*

ABSTRACT

The Diavik Waste Rock Project consists of laboratory scale and field scale experiments with one of its primary goals being the development of scale-up techniques for the prediction of impacts from mine wastes on groundwater and surface water. As part of the Diavik project, humidity cell experiments have been conducted to assess the long term geochemical evolution of the low sulfide content waste rock. Reactive transport modelling has been used to assess the significant geochemical processes controlling oxidation of sulfide minerals and subsequent sulfate and metals release from the humidity cell experiments. The geochemical evolution of effluent from waste rock with sulfide content of 0.16 wt. % (primarily pyrrhotite) in a subset of the humidity cells was simulated with the reactive transport model MIN3P under the conceptual model of constant water flow and that sulfide oxidation is controlled by the availability of ferric iron. Elevated metal concentrations in the humidity cell effluent were released through sulfide oxidation, which is controlled by diffusion of ferric iron to the unreacted particle surface and aerobic oxidation of the released ferrous iron. Elevated sulfate concentrations in solution are influenced by the production of intermediary sulfur compounds (represented in the model by S^0). Comparison of humidity cell experiments containing rock of varying sulfide content and temperature indicate available surface area and temperature also play important roles in rates of sulfide oxidation and subsequent sulfate production. The simulations also indicate that secondary mineral formation affects solute release. The humidity cell simulations are intended to provide a baseline for future reactive transport simulations of the larger scale field experiments at the Diavik site.

Keywords: sulfide oxidation, shrinking core model, reactive transport

INTRODUCTION

An important component of the planning of a mining project is the prediction of waste-rock effluent quality. The potential for mine waste rock to generate acid and elevated solute concentrations in effluent and the associated long term effects to the surrounding environment are often characterized using laboratory scale humidity cell experiments (Lapakko, 2003; Ardau, Blowes & Ptacek, 2009; Sapsford et al., 2009). The subsequent prediction process commonly involves the extrapolation of contaminant leaching rates derived from humidity cell experiments using empirical scale factors. The resulting scaled leaching rates are used to assess the potential for poor quality effluent from full scale waste-rock piles (commonly referred to as scale-up). Scale factors often include parameters understood to influence effluent quality such as pH, grain size, moisture content, temperature, oxygen availability and mineral surface area and volume (Kempton, 2012). The empirical scale factor method is often rendered incapable of accurate effluent quality prediction since site specific heterogeneities that arise during scale-up such as variability in flow mechanisms and geochemical reaction mechanisms are difficult to model given the simplified parameters. Reactive transport modelling has the potential to address some of the complexities associated with scale-up by providing a detailed, mechanistic, and quantitative approach to assessing effluent quality that encompasses the capability to take site specific processes into consideration.

The reactive transport model MIN3P (Mayer, Frind & Blowes, 2002) is used to simulate the weathering of waste rock to allow assessment of the primary geochemical processes involved. This article presents a conceptual model of pyrrhotite weathering in low S waste rock using the results of humidity cell effluent quality sampling and the resulting estimated weathering rate, and mineralogical and hydraulic properties from the humidity cell experiments and field scale experiments. The simulations are intended to provide a comprehensive geochemical conceptual model that will later be included in modelling of larger scale field experiments.

HUMIDITY CELL METHODOLOGY

As part of the Diavik Waste Rock Project (DWRP), 36 humidity cell experiments were conducted at the University of Waterloo over a period of approximately six years using representative run of mine waste rock collected at Diavik Diamond Mine (Diavik). The experiments were designed to assess the primary geochemical mechanisms controlling effluent quality from waste rock piles at the mine site. The primary sulfide mineral present in the waste rock is pyrrhotite wherein minor substitution of Ni and Cu for Fe has occurred in the following approximate ratio: [$Fe_{0.852}Ni_{0.004}Co_{0.001}S$] (Jambor, 1997). Given the relatively low sulfide content of the waste rock, the humidity cell experiments were used to assess the potential for acid generation as well as increased concentrations of solutes such as sulfate [SO_4], Fe, Ni, Cu, and Zn.

The Diavik waste rock used in the humidity cell experiments was collected in 2004 and 2005 and includes approximately 75 % granite (primarily quartz [SiO_2], k-feldspar [$KAlSi_3O_8$], and albite [$NaAlSi_3O_8$]), 14 % pegmatitic granite, 10 % biotite schist, and 1 % diabase (Blowes & Logsdon, 1998; Langman et al., 2014). The biotite schist is composed primarily of albite (35–55 %), quartz (20–50 %), and biotite [$KMg_2FeAlSi_3O_{10}(OH)_2$] (10–25 %) and contains a mean sulfide content of 0.24 wt. % S (Langman et al., 2014). Static testing was conducted on each of the humidity cell samples to determine S and C content (Langman et al., 2014). Other sulfide minerals present in the waste rock include minor amounts of chalcopyrite [$CuFeS_2$], sphalerite [ZnS], and pentlandite [$(Ni,Fe)_9S_8$]. The

waste rock is sorted into three types according to sulfur content (Type I < 0.04 wt. %, Type II 0.04 to 0.08 wt. %, and Type III > 0.08 wt. % S) (Smith et al., 2013).

Each humidity cell contained 1 kg of Type I, Type II, or Type III waste rock, through which deionized water was flushed at a rate of 500 mL·wk^{-1}. Once per week water was added to the cells and held for approximately one hour then allowed to drain from the cells. Draining of the cells typically lasted four to six hours and was followed by periods of dry air flow (three days at < 10 % relative humidity) and humid air flow (three days at > 95 % relative humidity) lasting the remainder of the week (Langman et al., 2014). The experiments followed the American Society for Testing and Materials (ASTM) method for humidity cell testing (ASTM, 1996) with increased flooding in the early stages according to the ASTM method modification described by Lapakko and White (2000). Duplicate sets of humidity cell experiments were conducted at two control temperatures (one set at approximately 22 °C and one set at approximately 5 °C).

CONCEPTUAL MODEL

The conceptual model presented here was based on the Type III (sulfide content of 0.16 wt. %), room temperature humidity cell experiments conducted as part of the DWRP and described by Langman et al., 2014. Because of the abundance of oxygen and moisture in the system, sulfide oxidation has been posited to be the significant geochemical process contributing to elevated concentrations of sulfate, Ni, and Co in the humidity cell effluent. Water flow through the model domain is described as continuous infiltration at a rate of 500 mL·wk^{-1}. Although the addition of water to the cells was conducted as flooding events (i.e. 500 mL over the period of a few hours), continuous infiltration was assumed to be a reasonable approximation because weekly flooding and limited evaporation during the dry air influx period did not likely result in significant moisture content reduction.

The oxidation of pyrrhotite was represented by a series of three primary reactions designed to simulate the reaction pathways for sulfide mineral oxidation outlined by Schippers & Sand (1999) and Rohwerder et al. (2003). Following the reaction mechanism for sulfide oxidation, ferric iron was considered as the dominant sulfide oxidizer according to the following overall reaction (Nicholson & Scharer, 1998; Janzen, Nicholson & Scharer, 2000; Belzile et al., 2004):

$$Fe_{(1-x)}S + (8-2x)Fe^{3+} + 4H_2O \rightarrow (9-3x)Fe^{2+} + SO_4^{2-} + 8H^+ \quad (1)$$

The reaction mechanism presented by Schippers & Sand (1999) and Rohwerder et al. (2003) includes the polysulfide pathway wherein several partially oxidized S species (primarily S^0 in the absence of sulfur oxidizing bacteria) can be produced as the reaction sequence progresses towards the fully oxidized product SO_4. The polysulfide pathway is appropriate for the oxidation of monosulfides such as pyrrhotite (Schippers & Sand, 1999; Rohwerder et al., 2003). Elemental S was selected as a proxy for the intermediary components in the MIN3P simulations. Introducing S^0 as an intermediary component results in the following reaction sequence (Nicholson & Scharer, 1998) where equation 2 represents an oxidation process and equation 3 represents an oxidation and dissolution process:

$$Fe_{(1-x)}S + (2-2x)Fe^{3+} \rightarrow (3-3x)Fe^{2+} + S^0 \quad (2)$$

$$S^0 + 1.5O_{2(aq)} + H_2O \rightarrow SO_4^{2-} + 2H^+ \quad (3)$$

Equations 2 and 3 were ultimately driven in the simulations by the oxidation of Fe^{2+}, facilitating the replenishment of Fe^{3+} represented by the following reaction (Singer & Stumm, 1970; Schippers & Sand, 1999; Rohwerder et al., 2003):

$$Fe^{2+} + 0.25O_{2(aq)} + H^{+} \leftrightarrow Fe^{3+} + 0.5H_2O \quad (4)$$

The rate of sulfide oxidation (equation 2) was simulated using the shrinking core model (Levenspiel, 1972; Wunderly et al., 1996; Mayer, Frind & Blowes, 2002) and was represented in the model using the following rate expression (after Mayer, Frind & Blowes, 2002):

$$R_{Po\ ox} = -10^3 S_{Fe_{0.852}Ni_{0.004}Co_{0.001}} \left[\frac{r^p}{(r^p - r^r)r^r}\right] D_{Fe^{3+}} \left[\frac{Fe^{3+}}{1.714}\right] \quad (5)$$

where $R_{Po\ ox}$ represents the rate of pyrrhotite oxidation using the shrinking core model [mol·L^{-1}·d^{-1}] and $S_{Fe_{0.852}Ni_{0.004}Co_{0.001}}$, r^p, r^r, and $D_{Fe^{3+}}$represent the reactive surface area [m^2 mineral·dm^{-3} porous medium], average particle radius [m], unreacted particle radius [m], and effective diffusion coefficient [m^2·s^{-1}] of Fe^{3+} to the unreacted surface, respectively.

In addition to chemical oxidation processes, microbial populations play an important role in the oxidation of sulfide minerals (Nordstrom & Southam, 1997; Blowes et al., 2003). Most probable number bacteria count data from the DWRP humidity cell experiments (Langman et al., 2014) indicates that neutrophilic sulfur oxidizing bacteria (nSOB) were the dominant microbiological catalyst in the system. As a result, biotic oxidation was represented in the rate expressions associated with equations 3 and 4 by simulating the increase in reaction rate with increasing substrate (in this case Fe^{2+} and S^0) concentration to represent the increase in microbial activity.

The rate of ferric iron production (equation 4) was simulated using the rate expression (after Singer & Stumm, 1970; Mayer, Frind & Blowes, 2002; Roden, 2008):

$$R_{Fe^{2+}-Fe^{3+}} = -S\left[k^1_{Fe^{2+}-Fe^{3+}}[Fe^{2+}][O_{2(aq)}] + k^2_{Fe^{2+}-Fe^{3+}}[Fe^{2+}][O_{2(aq)}][OH^-]^2\right]$$
$$-k^3_{Fe^{2+}-Fe^{3+}}\left[\frac{[Fe^{2+}]}{K_s+[Fe^{2+}]}\right] \quad (6)$$

The first two terms in equation 6 represent the chemical oxidation of Fe^{2+} by aqueous oxygen where $R_{Fe^{2+}-Fe^{3+}}$ represents the rate of Fe^{2+} oxidation [mol·L^{-1}·d^{-1}] and S, $k^1_{Fe^{2+}-Fe^{3+}}$, and $k^2_{Fe^{2+}-Fe^{3+}}$ represent a scaling factor [-], the reaction rate constant for pH < ~ 3.5 [L·mol^{-1}·d^{-1}] (Singer & Stumm, 1970), the reaction rate constant for pH > ~ 4.5 [mol·L^{-1}·d^{-1}] (Singer & Stumm, 1970), respectively. The third term in equation 6 represents the biotic oxidation of Fe^{2+} by microbes where $k^3_{Fe^{2+}-Fe^{3+}}$ and K_s represent the reaction rate constant [mol·L^{-1}·d^{-1}] and half-saturating constant [mol·L^{-1}], respectively.

Sulfate concentrations in humidity cell effluent were simulated by the bioitic oxidation of S^0 to SO_4 according to the reaction stoichiometry in equation 3. The rate of S^0 oxidation is dependent on the presence of both oxygen and the S^0 however, due to the abundance of oxygen in the system only S^0 is represented in the following rate expression (after Roden, 2008):

$$R_{S^0-SO_4} = -k_{S^0-SO_4}\left[\frac{[S^0]}{K_s+[S^0]}\right] \quad (7)$$

where $R_{S^0-SO_4}$represents the rate of biotic S^0 oxidation by [mol·L^{-1}·d^{-1}] and $k_{S^0-SO_4}$and K_s represent

the reaction rate constant [mol·L^{-1}·d^{-1}] and half-saturating constant [mol·L^{-1}] respectively.

Minor constituent sulfide minerals chalcopyrite, sphalerite, and pentlandite, were also included in the simulations undergoing oxidation by Fe^{3+} according to the shrinking core model (equation 5, Table 1). Additional primary minerals were simulated to dissolve as surface controlled reactions (Table 1) according to pH dependent (calcite, biotite, muscovite, and albite) or transition state rate expression (k-feldspar and quartz).

Secondary minerals (primarily iron-bearing oxides and hydroxysulfates) are expected to precipitate in association with the oxidation of sulfide minerals (Blowes et al., 2003; Jambor, 2003). Several secondary minerals were added to the system based on saturation index analysis conducted using Type III, room temperature humidity cell effluent chemistry data in conjunction with the geochemical speciation software PHREEQC (Parkhurst & Appelo, 1999). The saturation index analysis indicated that minerals ferrihydrite [$Fe(OH)_3$], jarosite [$KFe_3(SO_4)_2(OH)_6$], and gibbsite [$Al(OH)_3$] were supersaturated in the humidity cell effluent at various points of the experiments. These minerals were allowed to precipitate or dissolve during the simulations according to equilibrium controlled rate expressions. Amorphous silica [$SiO_{2(am)}$] was also allowed to precipitate according to an equilibrium controlled rate expression to prevent excess Si build up.

Table 1 Reaction stoichiometry used in sulfide weathering simulations

Mineral	Primary Minerals	log K
(1) pyrrhotite	$Fe_{0.852}Ni_{0.004}Co_{0.001}S + 1.714Fe^{3+} \rightarrow 2.566Fe^{2+} + 0.004Ni^{2+} + 0.001Co^{2+} + S^0$	--
(2) sphalerite	$ZnS + 2Fe^{3+} \rightarrow 2Fe^{2+} + Zn^{2+} + S^0$	--
(3) chalcopyrite	$FeCuS_2 + 4Fe^{3+} \rightarrow 5Fe^{2+} + Cu^{2+} + 2S^0$	--
(4) pentlandite	$Fe_{4.5}Ni_{3.6}Co_{0.9}S_8 + 18Fe^{3+} \rightarrow 22.5Fe^{2+} + 3.6Ni^{2+} + 0.9Co^{2+} + 8S^0$	--
(5) calcite	$CaCO_3 \rightarrow Ca^{2+} + CO_3^{2-}$	-8.48
(6) biotite	$KMg_2Fe(AlSi_3O_{10})(OH)_2 + 10H^+ \rightarrow K^+ + 2Mg^{2+} + Fe^{2+} + Al^{3+} + 3H_4SiO_4$	--
(7) muscovite	$KAl_2(AlSi_3O_{10})(OH)_2 + 10H^+ \rightarrow K^+ + 3Al^{3+} + 3H_4SiO_4$	--
(8) k-feldspar	$KAlSiO_8 + 4H_2O + 4H^+ \rightarrow K^+ + Al^{3+} + 3H_4SiO_4$	0.08
(9) albite	$NaAlSi_3O_8 + 4H_2O + 4H^+ \rightarrow Na^+ + Al^{3+} + 3H_4SiO_4$	--
(10) quartz	$SiO_2 + 2H_2O \rightarrow H_4SiO_4$	-3.98
	Secondary Minerals	
(11) ferrihydrite	$Fe(OH)_{3(am)} + 3H^+ \leftrightarrow Fe^{3+} + 3H_2O$	4.89
(12) jarosite	$KFe_3(SO_4)_2(OH)_6 + 6H^+ \leftrightarrow K^+ + 3Fe^{3+} + 2SO_4^{2-} + 6H_2O$	-9.21
(13) silica (am)	$SiO_{2(am,gl)} + 2H_2O \leftrightarrow H_4SiO_4$	-3.02
(14) gibbsite	$Al(OH)_{3(am)} + 3H^+ \leftrightarrow Al^{3+} + 3H_2O$	8.11

Table 2 Stoichiometry used in intra-aqueous reactions

Primary Components	Intra-aqueous Reactions	log K
(1) Fe(II)/Fe(III)	$Fe^{2+} + 0.25O_{2(aq)} + H^+ \leftrightarrow Fe^{3+} + 0.5H_2O$	--
(2) SO_4^{2-}/HS-	$HS^- + 2O_{2(aq)} \leftrightarrow SO_4^{2-} + H^+$	-138.38
(3) S^0- SO_4^{2-}	$S^0 + 1.5O_{2(aq)} + H_2O \rightarrow SO_4^{2-} + 2H^+$	--

MODEL PARAMETERS

The humidity cell experiments were conducted in cylinders with diameter of approximately 0.1 m resulting in an average height of waste rock of 0.1 m. Flow through the humidity cells was simulated as a 1-D column with the vertical domain set at 0.1 m, discretized into 100 1 mm control volumes. The simulations were run for a 2240 d period corresponding approximately to the data set available as of September 2014. Because atmospheric air (humidity adjusted) was used for the air flow portions of the experiment and the infiltrating deionized water was not isolated from atmospheric conditions, the cells were assumed to be in equilibrium with atmospheric oxygen and carbon dioxide at all times. The temperature of the simulations was set at 22 °C to be consistent with the conditions of the experiments. Flow parameters (Table 3) including porosity, hydraulic conductivity, and soil hydraulic function parameters were based on the work of Neuner et al., 2013 or by analysis of humidity cell data; dispersivity along the 0.1 m flow path was ignored. Mineral weight percent (Table 4) for pyrrhotite, calcite, biotite, muscovite, k-feldspar, albite, and quartz were calculated based on the general waste rock content documented by Jambor (1997), with values for chalcopyrite and sphalerite estimated from the molar ratios of Cu^{+2} and Zn^{+2} to Ni^{+2} in humidity cell effluent. The resulting estimates for the weight percent of chalcopyrite and sphalerite were consistent with values estimated by Bailey (2013). The weight percent for pentlandite was calibrated as part of the simulations. The initial volume fractions of secondary minerals expected to precipitate were set to an arbitrary low value (i.e. 1 x 10^{-10}).

Table 3 Physical parameters used in simulations

Parameter		Value
hydraulic conductivity ($m \cdot s^{-1}$)		2.5 x 10^{-4}
van Genuchten soil hydraulic parameters	α (m^{-1})	8.8
	n	1.7
flow rate ($m \cdot s^{-1}$)		1.0 x 10^{-9}
Porosity		0.26

Table 4 Composition of waste rock

Mineral	wt. %
pyrrhotite	0.17[1]
chalcopyrite	0.01[1]
sphalerite	0.01[1]
pentlandite	0.01[1]
calcite	0.07[1]
biotite	7.0[2]
muscovite	2.3[2]
k-feldspar	38.0[2]
albite	20.3[2]
quartz	30.4[2]

[1]Based on results of static testing with adjustment during calibration phase of model.

[2]Based on results of Jambor 1997

Dissolution and precipitation reactions involving primary minerals were kinetically controlled and irreversible (with the exception of calcite, which was simulated as a reversible reaction). Secondary mineral precipitation and dissolution reactions were kinetically controlled and reversible.

RESULTS AND DISCUSSION

To evaluate the conceptual model and assess the resulting simulations, the output of the MIN3P simulations were optimized for best fit to measured effluent concentrations of selected solute parameters from the Type III, room temperature humidity cells. All hydraulic parameters were fixed during the optimization process. Initial elevated concentrations of SO_4 and cations were not considered since they were likely a result of the initial blasting process (Bailey et al., 2013). Subsequent to the initial flush of blasting residuals, measured solute concentrations increased from relatively low concentrations to peak concentrations over a period of ten to approximately 24 weeks depending on the parameter (SO_4 concentrations peaked at approximately ten weeks whereas Ni^{2+} and Co^{2+} concentrations peaked at approximately 24 weeks).

To assess the general applicability of the simulations to other humidity cells and field scale experiments, the simulated rate of sulfide oxidation was compared to the rate of sulfide oxidation for the Type III waste rock calculated using the concentrations of SO_4 in the Type III, room temperature humidity cell effluent by Langman et al. (2014) (Figure 1). The good fit over most of the simulated period indicates that the model captures the general rate of oxidation suggesting a reasonable approximation of the overall sulfide oxidation process at the laboratory scale.

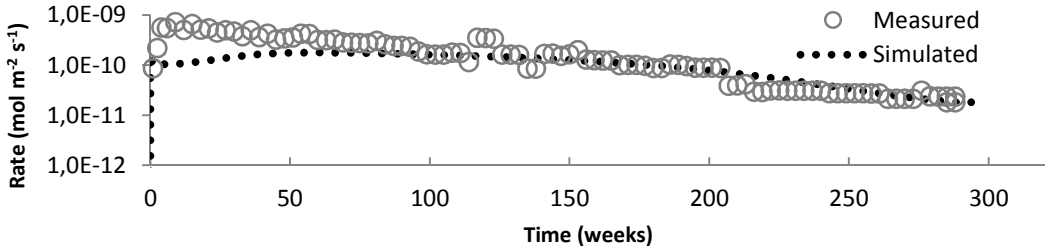

Figure 1 Rate of sulfide oxidation [mol·m^{-2}·s^{-1}] versus time [weeks] as estimated from measured SO_4 concentrations in humidity cell effluent compared to MIN3P sulfide oxidation simulation results

To assess specific processes, the measured effluent concentrations of SO_4,Ni^{2+}, and Co^{2+} from the Type III humidity cells are compared to the simulation results (Figure 2). The effective rate constants for non-sulfide minerals were used to calibrate the simulations to allow best fit to the measured effluent chemistry data. For sulfide minerals, the reactive surface area was used to calibrate the simulations.

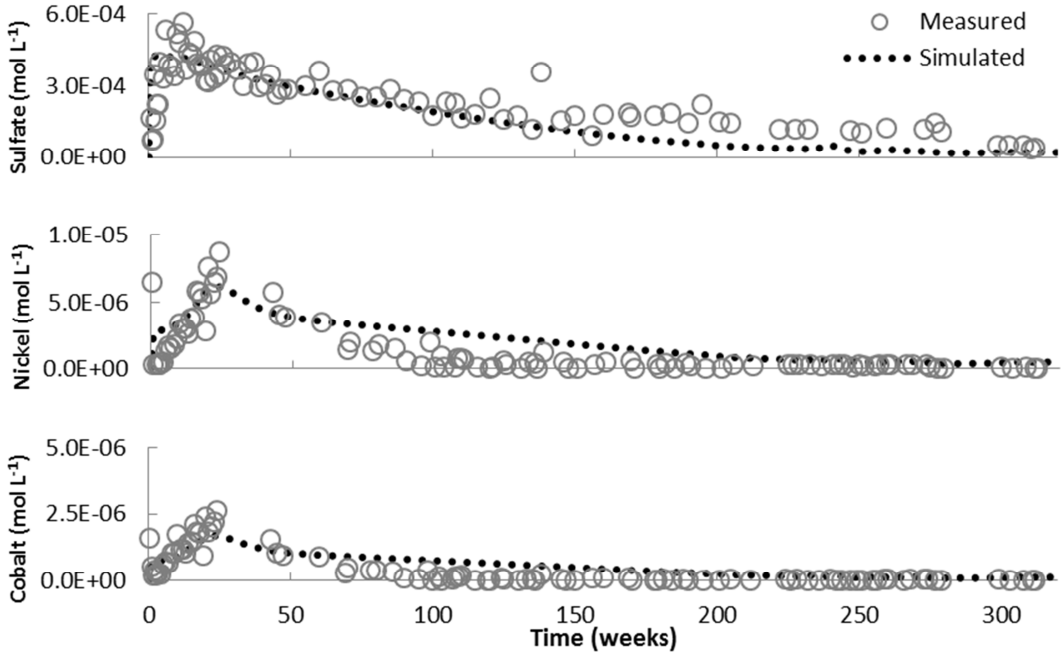

Figure 2 Concentrations of sulfide oxidation products SO_4, Ni^{2+}, and Co^{2+} [mol·L^{-1}] versus time [weeks] measured in humidity cell effluent compared to aqueous concentrations exiting the simulation domain

Simulated sulfate concentrations show a good fit to the measured data throughout the modelled period indicating an initial increase to peak concentrations at approximately ten weeks followed by a monotonic decrease. These trends are simulated through changes in the rates of microbially mediated oxidation reactions and available reactive surface area, as described by the shrinking core model.

Simulated Ni^{2+} and Co^{2+} concentrations followed a pattern generally similar to SO_4, with peak concentrations occurring slightly later than the sulfate concentration peak (Ni^{2+} and Co^{2+} concentrations peaked at about 24 weeks). The later peak concentrations of cations are attributed to slower oxidation rates for pentlandite when compared to the oxidation rate of pyrrhotite.

CONCLUSIONS

The general agreement between the simulated solute concentrations and the measured humidity cell concentrations indicates a reasonable conceptual geochemical model has been put forward for the oxidation of sulfides contained in Diavik waste rock. The major components controlling oxidation of the sulfide minerals were identified by the modelling study to be the biotic influence on the rate of S^0 oxidation and the available reactive surface area of sulfide minerals. Further work is required to identify the major controls on iron concentrations and biotite dissolution rates, which will facilitate use of the geochemical conceptual model for the field scale experiments that are part of the DWRP.

ACKNOWLEDGEMENTS

Funding for this research was provided by a Collaborative Research and Development Grant from the Natural Sciences and Engineering Research Council of Canada (NSERC) awarded to D.W. Blowes, Principal Investigator; Diavik Diamond Mines, Inc.; the International Network for Acid Prevention; and the Mine Environment Neutral Drainage Program.

NOMENCLATURE

$\boldsymbol{R_{Po\ ox}}$	rate of pyrrhotite oxidation
$S_{Fe_{0.852}Ni_{0.004}Co_{0.001}}$	reactive surface area
r^p	average particle radius
r^r	unreacted particle radius
$D_{Fe^{3+}}$	effective diffusion coefficient of Fe^{+3} to the unreacted surface
$\boldsymbol{R_{Fe^{2+}-Fe^{3+}}}$	rate of Fe^{+2} oxidation
$k^1_{Fe^{2+}-Fe^{3+}}$	reaction rate constant for pH < ~ 3.5
$k^2_{Fe^{2+}-Fe^{3+}}$	reaction rate constant for pH > ~ 4.5
S	scaling factor
$k^3_{Fe^{2+}-Fe^{3+}}$	reaction rate constant
K_s	half saturating constant
$\boldsymbol{R_{S^0-SO_4}}$	rate of S^0 oxidation
$\boldsymbol{k}_{S^0-SO_4}$	reaction rate constant

REFERENCES

American Society for Testing and Materials. *Test Method for Laboratory Weathering of Solid Materials Using a Humidity Cell*; ASTM International, 1996; p. 19.

Ardau, C., Blowes, D.W., Ptacek, C.J., 2009. Comparison of laboratory testing protocols to field observations of the weathering of sulfide-bearing mine tailings. J. Geochem. Explor. 100, 182-191.

Bailey, B.L., Smith, L.J.D., Blowes, D.W., Ptacek C.J., Smith, L., Sego, D.C., 2013. The Diavik Waste Rock Project: Persistence of contaminants from blasting agents in waste rock effluent. App. Geochem., Vol. 36, pp 256-270.

Bailey, B.L., 2013. Geochemical and microbiological characterization of effluent and pore water from low-sulfide content waste rock. Ph.D. thesis, University of Waterloo, 399 p.

Belzile, N., Chen, Y.W., Cai, M.F., Li, Y., 2004. A review on pyrrhotite oxidation. J. Geochem. Explor. 84, 65–76.

Blowes, D.W., Logsdon, M.J., 1998. Diavik geochemistry baseline report. Prepared by Sala Groundwater, Inc. and Geochimica, Inc. for Diavik Diamond Mines and submitted to Canadian Environmental Assessment Agency, 121 p.

Blowes, D.W., Ptacek, C.J., Jambor, J.L., Weisener, C.G., 2003. The geochemistry of acid mine drainage. In: Lollar, B.S. (Ed.), Environmental Geochemistry, 9, Treatise on Geochemistry, Elsevier-Pergamon, pp. 149–204.

Jambor, J.L., 1997. Mineralogy of the Diavik Lac de Gras kimberlites and host rocks. Prepared by Leslie Investment, Ltd. for Diavik Diamond Mines and submitted to the Canadian Environmental Assessment Agency, 1997, 187 p.

Jambor, J.L., 2003. Mine-waste mineralogy and mineralogical perspectives of acid-base accounting. In: Jambor, J.L., Blowes, D.W., Ritchie, A.I.M. (Eds.), Environmental Aspects of Mine Wastes: Mineralogical Association of Canada Short Course Series. Economic Geology Publishing Company, pp. 117-145.

Janzen, M.P., Nicholson, R.V., Scharer, J.M., 2000. Pyrrhotite reaction kinetics: reaction rates for oxidation by oxygen, ferric iron, and for nonoxidative dissolution, Geo. Cos. Acta 64(9), 1511–1522.

Kempton, H., 2012, A review of scale factors for estimating waste rock weathering from laboratory tests: International Conference on Acid Rock Drainage (ICARD) Ottawa, 9th, Canada, 20–24 May 2012, Proceedings.

Lapakko, K.A., 2003. Developments in humidity-cell tests and their application. In: Jambor, J.L., Blowes, D.W., Ritchie, A.I.M. (Eds.), Environmental Aspects of Mine Wastes: Mineralogical Association of Canada Short Course Series. Economic Geology Publishing Company, pp. 147-164.

Lapakko, K.A., White, W.W., 2000. Modification of the ASTM 5744-96 kinetic test. In *Proceedings of Fifth International Conference on Acid Rock Drainage*; Society for Mining, Metallurgy, and Exploration: Littleton, Colorado, 2000; pp. 631–639.

Langman, J.B., Moore, M.L., Ptacek, C.J., Smith, L., Sego, D., Blowes, D.W., 2014. Diavik Waste Rock Project: evolution of mineral weathering, element release, and acid generation and neutralization during a 5-year humidity cell experiment. Minerals 4(2), 257–278.

Levenspiel, O., 1972. Chemical Reaction Engineering, 2nd ed., John Wiley & Sons, New York, 361–371.

Mayer, K.U., Frind, E.O., Blowes, D.W., 2002. Multicomponent reactive transport modeling in variably saturated porous media using a generalized formulation for kinetically controlled reactions. Water Resour. Res. 38(9), 13-1–21.

Neuner, M., Smith, L., Blowes, D.W., Sego, D.C., Smith, L.J.D., Fretz, N., Gupton, M., 2013. The Diavik Waste Rock Project: water flow though waste rock in a permafrost terrain. Appl. Geochem. 36, 222–233.

Nicholson, R.V., Scharer, J.M., 1998. Laboratory Studies of Pyrrhotite Oxidation, MEND Project 1.21.2.

Nordstrom, D.K., Southam, G., 1997. Geomicrobiology of sulfide mineral oxidation. Rev. Mineral. Geochem. 35, 361–390.

Parkhurst, D.L., Appelo, C.A.J., 1999. *PHREEQCi (version 2)* – A computer program for speciation, batch reaction, one dimensional transport, and inverse geochemical calculations: U.S. Geological Survey Water-Resources Investigations.

Roden, E.E., 2008. Microbiological Control on Geochemical Kinetics 1: Fundamentals and Case Study on Microbial Fe(III) Oxide Reduction. In: Brantley, S.L., Kubicki, J.D., White, A.F. (Eds.), Kinetics of Water-Rock Interaction. Springer Science+Business Media, pp. 335-415.

Rohwerder, T., Gehrke, T., Kinzler, K., Sand, W., 2003. Bioleaching review part A: Progress in bioleaching: fundamentals and mechanisms of bacterial metal sulfide oxidation. Appl. Microbiol. Biotechnol. (2003) 63: 239-248.

Sapsford, D.J., Bowell, R.J., Dey, M., Williams, K.P., 2009. Humidity cell tests for the prediction of acid rock drainage. Minerals Engineering, Vol. 22, pp. 25-36.

Schippers, A., Sand, W., 1999. Bacterial leaching of metal sulfides proceeds by two indirect mechanisms via thiosulfate or via polysulfides and sulfur. Appl. Environ. Microbiol. 65(1), 319–321.

Singer P.C., Stumm, W., 1970. Acidic Mine Drainage : The Rate-Determining Step. Science, New Series, Vol. 167, No. 3921 (Feb. 20, 1970), pp. 1121-1123.

Smith, L.J.D., Bailey, B.L., Blowes, D.W., Jambor, J.L., Smith, L., Sego, D.C., 2013. The Diavik Waste Rock Project: initial geochemical response from a low sulfide waste rock pile. Appl. Geochem. 36, 210–221.

Wunderly, M.D., Blowes, D.W., Frind, E.O., Ptacek, C.J., 1996. Sulfide mineral oxidation and subsequent reactive transport of oxidation products in mine tailings impoundments: A numerical model. Water Resour. Res. 32, 3173–3187.